C. 1

NACA

RESEARCH MEMORANDUM

EXPERIMENTAL INVESTIGATION OF AIR-COOLED TURBINE BLADE IN TURBOJET ENGINE

VIII - ROTOR BLADES WITH CAPPED LEADING EDGES

By Gordon T. Smith and Robert O. Hickel

Lewis Flight Propulsion Laboratory
Cleveland, Ohio

NATIONAL ADVISORY COMMITTEE
FOR AERONAUTICS

WASHINGTON

UNCLASSIFIED October 18, 1951

NATIONAL ADVISORY COMMITTEE FOR AERONAUTICS

RESEARCH MEMORANDUM

EXPERIMENTAL INVESTIGATION OF AIR-COOLED TURBINE BLADE IN TURBOJET ENGINE

VIII - ROTOR BLADES WITH CAPPED LEADING EDGES

By Gordon T. Smith and Robert O. Hickel

SUMMARY

An air-cooled turbine blade having special provisions for cooling the leading edge of the blade by introducing air under a leading-edge cap was investigated in a modified production turbojet engine.

The cooling effectiveness was determined over a range of engine speed from 4000 to 11,350 rpm. The cooling-air flow per blade was varied from about 0.01 to about 0.1 pound per second. The results indicated effective cooling of the leading edge of the blade. For example, at an engine speed of 10,000 rpm, a coolant- to gas-flow ratio of 0.054, and an effective gas temperature of 1000° F, the leading-edge temperature was about 400° F, which is about 230° F cooler than the most effectively cooled leading-edge configuration previously investigated. The cooling-air pressure loss through the blade, based on coolant flow rate, was the lowest of any cooled-blade configuration so far investigated.

INTRODUCTION

A series of air-cooled turbine blade configurations are being investigated at the NACA Lewis laboratory under conditions of engine operation in order to obtain a blade configuration which will permit operation of blades fabricated from nonstrategic materials at current or higher inlet gas temperatures. The analytical and experimental research which preceded this program is reviewed in reference 1.

Previous investigations of three blade configurations (references 1 to 3) established that hollow blade shells containing tubes and fins in the coolant passage were characterized by severe chordwise temperature gradients. These configurations had well-cooled midchord regions but were as much as 500° F hotter at the leading and trailing edges of the blades than at the midchord. Analysis indicated that the high leading- and trailing-edge temperatures of these first blade

configurations might limit the operation of similar nonstrategic blades to inlet temperatures below those now in use. Consequently, a series of blade configurations featuring special modifications intended to reduce the large chordwise temperature variations were fabricated and investigated. The results of the investigation of the first six of these special configurations are presented in reference 4. These blades were designated as blades 4 to 9. Four more blades of this series, blades 11 to 14, are reported in reference 5. The results obtained with a split trailing edge (blade 10) intended to reduce the chordwise temperature gradient at the trailing edge of the blade are reported in reference 6. No effort was made to provide leading-edge cooling for this blade. The cooling effectiveness and pressure-loss characteristics of a blade with a capped leading edge intended to reduce the temperature gradient at the leading edge of the blade are herein compared with the results obtained for blades 8 and 9 of reference 4. This blade will hereinafter be called blade 15.

The cooled-blade temperature distribution of blade 15 was investigated over a range of constant engine speed from 4000 to 11,350 rpm. The cooling-air flow per blade was varied from about 0.01 to 0.1 pound per second at each engine speed.

SYMBOLS

The following symbols are used in this report:

N	engine speed (rpm)
p	static pressure (in. Hg absolute)
p'	total pressure (in. Hg absolute)
R	ratio of coolant flow per blade to combustion-gas flow per blade
r	radius (ft)
T	static temperature ($^{\circ}F$)
T'	total temperature ($^{\circ}F$)
w	weight flow rate (lb/sec)
η	efficiency of cooling-air compression in turbine wheel
ρ	density (slugs/cu ft)

φ temperature-difference ratio or cooling effectiveness $(T_{g,e} - T_B)/(T_{g,e} - T_{a,e,h})$

ω angular velocity of rotor (radians/sec)

Subscripts:

A combustion air

a blade cooling air

B cooled blade

c compressor

e effective

F fuel

g combustion gas

H rotor hub

h blade root

i inlet

m mixture of combustion gas and scavenge, bearing, and blade cooling air in tail pipe

T blade tip

0 NACA standard sea-level conditions

APPARATUS AND INSTRUMENTATION

Engine

The modified production turbojet engine used in this investigation was the same as that described in references 1 and 2 with the exception that the two cooled blades installed in the turbine rotor were of a different configuration. The blades immediately adjacent to the cooled blades were standard twisted rotor blades during most of the investigation.

The instrumentation on the engine was the same as that discussed in references 1 and 2 except for the location of the thermocouples on the air-cooled blades.

Blades

The cooled blade configuration investigated is shown in figure 1. The blade shell was of the same external configuration as blades 4, 5, and 7 to 9 of reference 4 and blade 10 of reference 6 except for the addition of a leading-edge cap. Before the installation of the leading-edge cap, holes of 0.0625-inch diameter were placed every 0.125 inch along the leading edge of the blade, (fig. 1(b)). A groove, perpendicular to the leading edge, was milled from each hole to a point about 0.125 inch rearward on both the pressure and suction surfaces of the blades. An Inconel sheet, formed to the contour of the leading edge, was then spot-welded to the lands between the milled slots. The rearmost edges of this leading-edge cap extended slightly beyond the ends of the milled slots and were raised about 0.030 inch from the blade surface in order to permit some distribution of cooling air to the areas between the slots. The leading-edge cooling-air passage was capped at the tip thus forcing the air in this passage to flow axially outward into the milled slots and then to discharge rearward to form a film of cool air on both the pressure and suction surfaces of the blades. The blade shell was fabricated from X-40, a high temperature alloy, and contained seven mild steel tubes which were Nicrobrazed to the blade shell. Five of the tubes were 0.156 inch in outside diameter and one tube was 0.125 inch in outside diameter. These six tubes had a wall thickness of approximately 0.012 inch. The remaining tube had an outside diameter of 0.250 inch and a wall thickness of about 0.020 inch. The blade shell and blade base were one integrally cast piece.

The location of the blade thermocouple instrumentation is schematically shown in figure 2. The spanwise temperature distribution at the leading edge of the cooled blades was measured by thermocouples A, B, C, and D. These thermocouples were located on the blade shell at the rear edge of the leading-edge cap. Thermocouples B and D were located symmetrically with respect to the leading edge in order to obtain temperatures at similar locations on the pressure and suction surfaces near the leading edge. This arrangement provided some indication as to whether the cooling air from beneath the leading-edge cap was being evenly distributed between the two blade surfaces. The chordwise temperature of the cooled blade was obtained at a point $2\frac{1}{2}$ inches from the blade tip and was measured by thermocouples G, H, I, and J, as indicated in figure 2. Thermocouple G was located on the leading edge between two of the cooling-air slots at the extreme leading edge of the Inconel cap. Thermocouples E and K measured the cooling-air

temperature at the inlet to the blade base for each of the cooled blades, as indicated in figure 2. Thermocouples F and L measured the uncooled blade temperature (effective gas temperature). The uncooled blade with thermocouple F was placed adjacent to the cooled blade with thermocouples A, B, C, and D, and the uncooled blade with thermocouple L was placed adjacent to the cooled blade with thermocouples G, H, I, and J.

PROCEDURE

Calculations

The calculation procedures used to reduce and correlate the data obtained during this investigation were the same as those required for previous investigations of this series and are explained in detail in references 1 to 3.

Experimental Procedure

The two cooled blades were placed in a cascade of nontwisted, hollow, uncooled blades in order to minimize the distortion of the combustion gas flow around the cooled blades (reference 1). A number of series of runs with varying test conditions were made in order to investigate the cooling effectiveness of the blades. For each series, the engine speed was held constant and the blade-cooling air was varied. Also, for each series a grouping of not more than six rotating thermocouples were connected because of the limitation of the thermocouple pickup system, which is described in reference 1.

The engine speed was increased in increments of 2000 rpm from 4000 to 10,000 rpm. Above 10,000 rpm, the engine speed was increased in increments of 500 rpm until an engine speed of 11,350 rpm was reached. At an engine speed of 10,000 rpm, one of the hollow uncooled blades failed and all of these blades were removed and replaced with standard twisted blades. Check runs were then made at 4000, 6000, and 8000 rpm to evaluate the effects of the twisted cascade on the heat transfer characteristics of the cooled blades. The investigation was then continued at engine speeds of 10,000 rpm and above, but at 10,500 rpm one of the cooled blades failed along a thermocouple groove just above the blade base. This blade was replaced by a standard, uncooled blade, which was shortened to reduce its weight and to maintain the dynamic balance of the rotor. The investigation was then continued at engine speeds of 10,500, 11,000, and 11,350 rpm with one cooled blade. For engine speeds up to 10,000 rpm, the cooling-air flow was varied from about 0.01 to 0.10 pound per second per blade. At engine speeds above 10,000 rpm, where the combustion gas temperature and centrifugal blade stress are relatively high, the minimum coolant flow was about 0.02 pound per second per blade.

A summary of conditions under which the investigation was conducted is given in table I.

RESULTS AND DISCUSSION

Blade Temperatures

Effect of cooling-air flow on blade, effective gas, and cooling-air temperatures. - An example of the basic temperature data taken during the investigation is shown in figure 3 for an engine speed of 10,000 rpm. Solid blade temperatures (effective gas temperatures), cooled blade temperatures and cooling-air temperatures are plotted against cooling-air-flow rate per blade. In general, the effective gas temperature remained essentially constant while the temperatures of the cooled blade and cooling air decreased with an increase in cooling-air flow. The temperature of the extreme leading edge of the blade cap (thermocouple G) was about 175° F cooler than the midchord temperatures (thermocouples H and J) over the entire range of coolant flows, as shown in figure 3(a). These low leading-edge temperatures represent very effective cooling of the leading edge of the blade because the midchord region of all blades previously investigated (references 1 to 6) have been considerably cooler than the leading and trailing edges, even on those blades having special leading- and trailing-edge cooling modifications. Thus, the leading-edge cap was clearly superior to all leading-edge cooling modifications previously investigated.

Two important disadvantages of previous cooled-blade designs have been overcome. Primarily, the temperature level of the leading-edge region has been reduced considerably. Secondly, a tendency for a rapid increase in leading-edge temperature with decreasing coolant flow for film-cooled blades previously investigated (references 4 and 5) has been eliminated as evidenced by the relatively slow rise in leading-edge temperature with a decrease in coolant flow shown by thermocouple G (fig. 3(a)) and thermocouples A, B, C, and D (fig. 3(b)).

Thermocouples B and D (fig. 2) were located symmetrically to the leading edge of the blade in order to obtain an indication of the relative distribution of the cooling-air film along the suction and pressure surfaces of the blades. The curves for thermocouples B and D (38-percent span) shown in figure 3(b) indicate that about the same amount of cooling air is flowing out along the pressure and suction surfaces of the blades as shown by the small differences in temperature throughout the entire range of coolant flows. This close agreement of the temperatures at B and D was observed over the entire range of engine speeds investigated.

The trailing-edge temperature (thermocouple I) of this blade is 140° to 260° F hotter than the midchord temperatures (thermocouples H and J), as shown in figure 3(a). No special attempt was made to cool the trailing-edge region of this blade, and consequently the trailing-edge temperatures are relatively high and compare closely in value with the trailing-edge temperatures of other blades previously investigated that had no special trailing-edge cooling (references 1 to 3).

The temperature trends of the capped leading-edge blade at lower engine speeds were similar to those shown for an engine speed of 10,000 rpm in figure 3.

The variation of temperature with coolant flow at an engine speed of 11,350 rpm is shown in figure 4 for thermocouples G, J, K, and L. These data are the first published temperature data near rated engine speed for this series of air-cooled turbine-blade investigations. As was the case at 10,000 rpm, the leading-edge temperature (thermocouple G) exhibited a much lower sensitivity to cooling-air flow rate than the leading-edge temperatures of the film-cooled blade which had been investigated at lower engine speeds. The change in temperature of thermocouple G with cooling-air flow rate was approximately the same as shown in figure 3(a) for an engine speed of 10,000 rpm. The change in temperature at the midchord (thermocouple J) for the engine speed of 11,350 rpm was also about the same as that for 10,000 rpm. The temperature level of thermocouples G and J was about 200° to 300° F higher at 11,350 rpm than at 10,000 rpm. This resulted essentially from an increase in effective gas temperature from about 1000° to 1360° F for an increase in engine speed from 10,000 to 11,350 rpm. The cooling-air temperature at the blade root was from 40° to 100° F higher at an engine speed of 11,350 rpm than at 10,000 rpm. Thermocouples I and J are not presented because they failed beyond repair at an engine speed of 10,500 rpm. Temperatures for the cooled blade having thermocouples A, B, C, and D along the leading edge are not presented because this blade failed along a thermocouple groove at an engine speed of 10,500 rpm.

Correlated cooled-blade temperatures. - The cooled-blade temperatures were correlated by use of the temperature-difference ratio $(T_{g,e} - T_B)/(T_{g,e} - T_{a,e,h})$, which is also referred to as φ or cooling effectiveness. The development and use of φ is discussed in detail in reference 1. The values of φ for the range of operating conditions in this investigation are summarized in table I. Series 1 to 5 of table I were made with the original nontwisted cascade of hollow uncooled blades adjacent to the cooled blades. Series 5 through 11 were made with standard twisted uncooled blades adjacent to the cooled blades. Comparison of the φ values obtained at like coolant flow rates for a given engine speed indicates that the pressure surface was cooler (higher φ values) and the suction surface was hotter (lower φ values) when the twisted blades were adjacent to the cooled blades. The temperatures along the leading edge, with the exception of thermocouple A, were not substantially affected. The changes in temperature of the midchord region were probably caused by the change in combustion gas flow area on either side of the cooled blades.

Blade Temperature Distribution Comparisons

In order to illustrate the cooling performance characteristics of the capped leading-edge blade, the chordwise temperature distribution of blade 15 is compared with blades 8 and 9 of reference 4 in figure 5. Blades 8 and 9 were selected for this comparison because both had what was previously regarded as well-cooled leading-edge sections. The chordwise temperature profile of a hypothetical blade consisting of a split trailing edge and capped leading edge is compared with the 10-tube blade of reference 1 in figure 6 in order to illustrate how effectively the chordwise temperature gradients have been relieved by the special modifications thus far investigated. The principal design characteristics of blades 8, 9, 15, and the composite blade are illustrated in figure 7.

Chordwise blade temperature comparisons. - A comparison of the chordwise temperature distribution of blade 15 with the chordwise temperature distributions of blades 8 and 9 is shown in figure 5. Blade 8 is more effectively cooled than blade 9; however, some doubt about the durability of blade 8 exists because of the large number of stress raising slots in the leading edge of the blade. The leading and trailing edges of blade 9 are cooled by a high-conductivity copper fin extending from the blade shell to copper tubes in the interior of the blade and blade 9 is thought to be structurally superior to blade 8. Both blades are shown because the service durability of blade 9 may equal or exceed that of blade 8. The comparison is for a coolant- to combustion-gas-flow ratio of 0.054, a cooling-air temperature at the blade root of 109° F, an effective gas temperature of 1000° F, and an engine speed of 10,000 rpm. The superiority of the leading-edge-capped blade in providing leading-edge cooling is clearly evident. The leading-edge temperature is about 230° F cooler than that of the most effectively cooled blade previously investigated. The temperature level of the leading edge was so effectively reduced that the temperature profile is inverted. As was previously mentioned, no special effort was made to provide trailing-edge cooling and consequently this region is quite hot. The midchord temperature on the pressure surface is about the same as that for blades 8 and 9. The midchord temperature on the suction surface, however, is about 70° to 130° F hotter than that for blades 8 and 9, respectively. Blades 8 and 9 were investigated in a cascade of nontwisted blades. The higher temperatures on the suction surface may have been the result of differences in gas flow around blade 15 caused by the use of twisted blades adjacent to blade 15. A combination of the capped leading-edge modification and an effective modification for cooling the trailing edge of the blade would appear to offer an effective air-cooled blade design.

A probable chordwise temperature-distribution comparison between a 10-tube blade and a hypothetical blade combining a split trailing edge, a reverse coolant flow path, and a capped leading edge is presented in figure 7. The assumption was made for the purpose of this comparison that the trailing-edge section received at least as great a proportion

of the total blade-cooling air as the trailing edge of blade 10 of reference 4 received. Incorporation of the reverse flow coolant path in the design would force all of the cooling air to be discharged either at the leading or trailing edge and this assumption would therefore probably be quite conservative. The curves of figure 6 were calculated using a cooling-air temperature of 109° F, an effective gas temperature of 1000° F, and a coolant- to gas-flow ratio of 0.05 for an engine speed of 10,000 rpm.

The original 10-tube blade had an effectively cooled midchord section but was very hot at the leading and trailing edges of the blade. The composite blade successfully reduced the high temperatures on the leading edge below the midchord temperatures of the 10-tube blade and succeeded in considerably reducing the trailing-edge temperature level. As a result, the average blade temperature and temperature gradients on the composite blade were much lower than on the 10-tube blade. This should result in a stronger blade with a reduced thermal stress level thus permitting increased engine performance through use of reduced coolant flow rates or increased turbine-inlet temperatures.

Spanwise blade temperature distribution. - The spanwise temperature distribution at the leading edge of blade 15 is shown in figure 8 at a coolant flow ratio of 0.05, a cooling-air inlet temperature at the blade root of 109° F, an effective gas temperature of 1000° F, and an engine speed of 10,000 rpm. A typical allowable temperature profile is also indicated to illustrate what is considered a nearly optimum blade temperature distribution. The temperature of blade 15 is highest at the blade tip and decreases rapidly along the span toward the blade root. The temperature reaches a minimum at about the one-third span position and then increases somewhat toward the blade root. This temperature variation corresponds reasonably well to the optimum temperature variation except for the rise in temperature in the neighborhood of the blade root.

Cooling-Air Pressure Losses

The cooling-air pressure loss from the rotor hub to the blade tip was calculated by the method presented in reference 2 from data taken at 4000, 6000, and 8000 rpm. No data were taken above 8000 rpm because it was necessary to use a special tail cone for the high speed runs which did not have the required instrumentation. The results of the measurements and calculations are presented as the upper curve of figure 9. The data for all engine speeds are well correlated up to a cooling-air weight flow of 0.07 pound per second per blade.

The pressure loss through the blade only, from root to tip, is shown on the lower curve in figure 9. This curve was obtained by subtracting the pressure loss from the rotor hub to the blade root from the loss from the rotor hub to the blade tip as described in reference 3. The pressure loss for blade 15 was the lowest of any cooled blade so far investigated.

A comparison of the pressure loss required to produce a given cooling effectiveness at the leading edge of blades 8, 9, and 15 is presented in figure 10. Blades 8 and 9 were selected for this comparison because they appeared to have a favorable combination of leading-edge cooling effectiveness and blade pressure loss. Apparently blade 15 provides by far the highest leading-edge cooling effectiveness for a given pressure loss. For example, at a pressure loss of 20 inches of mercury, blade 8 will provide a leading-edge cooling effectiveness of 0.23, blade 9 will provide an effectiveness of 0.39, while blade 15 will provide a cooling effectiveness at the leading edge of 0.686.

SUMMARY OF RESULTS

The important results of an experimental investigation of an air-cooled turbine blade having a capped leading edge were as follows:

1. The capped leading-edge configuration provided very effective cooling of the leading-edge portions of the blade. This configuration was clearly superior to the most effectively cooled leading-edge configurations previously investigated. For example, at an engine speed of 10,000 rpm, a coolant- to combustion-gas-flow ratio of 0.054, an effective gas temperature of 1000° F, and a cooling-air inlet temperature at the blade root of 109° F, the leading-edge temperature was about 400° F, approximately 230° F cooler than the most effectively cooled leading-edge configuration previously investigated.

2. The cooling-air pressure loss, based on coolant flow rate, was the lowest of any blade configuration as yet investigated.

Lewis Flight Propulsion Laboratory
National Advisory Committee for Aeronautics
Cleveland, Ohio

REFERENCES

1. Ellerbrock, Herman H., Jr., and Stepka, Francis S.: Experimental Investigation of Air-Cooled Turbine Blades in Turbojet Engine. I - Rotor Blades with 10 Tubes in Cooling-Air Passages. NACA RM E50I04, 1950.

2. Hickel, Robert O., and Ellerbrock, Herman H., Jr.: Experimental Investigation of Air-Cooled Turbine Blades in Turbojet Engine. II - Rotor Blades with 15 Fins in Cooling-Air Passages. NACA RM E50I14, 1950.

3. Hickel, Robert O., and Smith, Gordon T.: Experimental Investigation of Air-Cooled Turbine Blades in Turbojet Engine. III - Rotor Blades with 34 Steel Tubes in Cooling-Air Passages. NACA RM E50J06, 1950.

4. Ellerbrock, Herman H., Jr., Zalabak, Charles F., and Smith, Gordon T.: Experimental Investigation of Air-Cooled Turbine Blades in Turbojet Engine. IV - Effects of Special Leading- and Trailing-Edge Modifications on Blade Temperatures. NACA RM E51A19, 1951.

5. Arne, Vernon L., and Esgar, Jack B.: Experimental Investigation of Air-Cooled Turbine Blades in Turbojet Engine. VI - Conduction and Film Cooling of Leading and Trailing Edges of Rotor Blades. NACA RM E51C29, 1951.

6. Smith, Gordon T., and Hickel, Robert O.: Experimental Investigation of Air-Cooled Turbine Blades in Turbojet Engine. V - Rotor Blades with Split Trailing Edges. NACA RM E51A22, 1951.

TABLE I - SUMMARY OF ENGINE OPERATING CONDITIONS AND TEMPERATURE DIFFERENCE RATIOS FOR BLADE 15

Series	Engine speed N (rpm)	Effective gas temperature $T_{g,e}$ (°F)	Average conditions at compressor inlet: Total pressure $P_{A,c,i}$ (in. Hg abs.)	Average conditions at compressor inlet: Total temperature $T_{A,c,i}$ (°F)	Cooling-air flow per blade w_a (lb/sec)	Temperature difference ratio φ: Thermocouple A	B	C	D	Engine speed N (rpm)	Effective gas temperature $T_{g,e}$ (°F)	Average conditions at compressor inlet: Total pressure $P_{A,e,i}$ (in. Hg abs.)	Average conditions at compressor inlet: Total temperature $T_{A,c,i}$ (°F)	Cooling-air flow per blade w_a (lb/sec)	Temperature difference ratio φ: Thermocouple G	H	I	J
1	4,020 4,010 3,998 4,006 4,006 4,004 4,000 4,002 3,996 3,996 4,000	1013 1026 1076 1063 1089 1089 1080 1088 1095 1095 1095	26.84	75	0.0898 .0808 .0715 .0604 .0500 .0407 .0308 .0257 .0198 .0148 .0102	0.385 .388 .254 .251 .210 .188 .170 .157 .150 .144 .134	0.787 .795 .775 .766 .753 .737 .708 .694 .673 .681 .628	0.776 .770 .738 .718 .695 .670 .634 .620 .597 .579 .582	0.803 .795 .778 .770 .750 .720 .691 .671 .642 .615 .580	4,000 (Nominal)	1049 1058 1053 1052 1052	28.77	77	0.0708 .0601 .0508 .0444 .0347	0.745 .725 .634 .613 .566	0.618 .586 .480 .457 .406	0.333 .278 .250 .239 .212	0.666 .617 .532 .508 .429
2	5,998 5,996 5,998 5,996 5,998 6,012 6,002	1069 1075 1077 1073 1072 1074 1075	28.84	78	0.1010 .0715 .0508 .0308 .0248 .0199 .0100	0.341 .260 .208 .170 .166 .161 .128	0.804 .779 .744 .706 .694 .683 .641	0.773 .725 .678 .633 .621 .598 .553	0.797 .766 .721 .670 .653 .634 .576	6,000 (Nominal)	1045 1040 1045 1042 1048 1045	28.77	77	0.0715 .0601 .0514 .0196 .0148	0.787 .679 .628 .598 .561	0.551 .488 .432 .396 .344	0.288 .232 .202 .185 .168	0.609 .539 .484 .456 .435
3	8,006 8,002 8,010 7,996 7,994 8,006	1094 1094 1094 1090 1090 1092	29.08	84	0.0811 .0711 .0605 .0408 .0304 .0198	0.280 .245 .219 .205 .193 .171	0.784 .766 .735 .720 .702 .682	0.757 .699 .661 .645 .626 .598	0.754 .736 .686 .678 .655 .622	6,000 (Nominal)	1062 1072 1070 1068 1066	28.77	77	0.0810 .0716 .0602 .0311 .0201	0.728 .705 .654 .628 .587	0.518 .490 .447 .402 .358	0.222 .206 .188 .165 .160	0.586 .588 .518 .470 .432
4										10,004 9,996 10,002	1262 1260 1278	28.77	70	0.1002 .0810 .0714	0.715 .699 .664	0.486 .474 .440	0.215 .204 .190	0.556 .545 .510
5	4,000 (Nominal)	961 959 950	28.23	80	0.0897 .0601 .0324	0.487 .401 .310	0.826 .795 .724	0.786 .724 .625	0.830 .786 .704	4,005 4,005 4,005 4,000	952 956 951 951	28.18	80	0.0800 .0704 .0405 .0305	0.772 .747 .583 .552	0.718 .674 .548 .542	0.376 .348 .286 .261	0.834 .891 .803 .470
6	6,000 (Nominal)	900 900 901	29.25	80	0.0902 .0502 .0326	0.424 .355 .289	0.812 .775 .709	0.757 .683 .606	0.795 .752 .684	6,005 6,002 6,010 5,981	887 883 880 877	29.18	45	0.0806 .0710 .0408 .0306	0.750 .720 .658 .641	0.642 .604 .527 .498	0.297 .269 .230 .211	0.566 .522 .454 .427
7	8,000 (Nominal)	902 890 890	29.25	80	0.0901 .0801 .0326	0.375 .322 .266	0.787 .746 .706	0.726 .658 .610	0.758 .722 .662	7,969 7,993 7,993 7,993	868 887 872 862	29.18	50	0.0808 .0712 .0408 .0307	0.726 .702 .654 .633	0.577 .550 .502 .480	0.254 .241 .219 .209	0.522 .486 .430 .407
8	10,000 (Nominal)	1000 1000 998 998 998 995 998 994	29.25	80	0.0999 .0906 .0712 .0606 .0506 .0410 .0307 .0257	0.381 .348 .306 .280 .248 .225 .208 .199	0.745 .732 .695 .673 .650 .630 .608 .606	0.671 .650 .617 .601 .574 .590 .531 .527	0.736 .732 .700 .697 .668 .648 .637 .632	10,001 10,001 10,008 9,996 10,008 9,989 9,989 9,993	1005 1007 1007 1007 1000 1000 998 996	29.22	50	0.0995 .0899 .0805 .0708 .0601 .0500 .0407 .0307	0.819 .806 .674 .663 .641 .631 .611 .596	0.532 .520 .504 .492 .468 .448 .436 .403	0.245 .244 .238 .236 .228 .221 .212 .205	0.484 .476 .461 .451 .430 .416 .398 .384
9										10,500 10,488 10,502 10,500 10,496	1150 1260 1262 1260 1256	29.10	67	0.1020 .0824 .0617 .0298 .0208				0.438 .422 .406 .378 .371
10										11,022 11,008 11,016 10,994 10,984	1332 1321 1320 1340 1350	29.10	70	0.1030 .0826 .0617 .0302 .0156				0.478 .453 .428 .356 .341
11										11,366 11,362 11,356 11,354 11,552 11,346 11,348	1365 1360 1360 1358 1361 1360 1360	29.10	70	0.1027 .0816 .0622 .0729 .0496 .0501 .0204	0.648 .636 .622 .613 .598 .584 .568			0.438 .421 .414 .401 .380 .356 .331

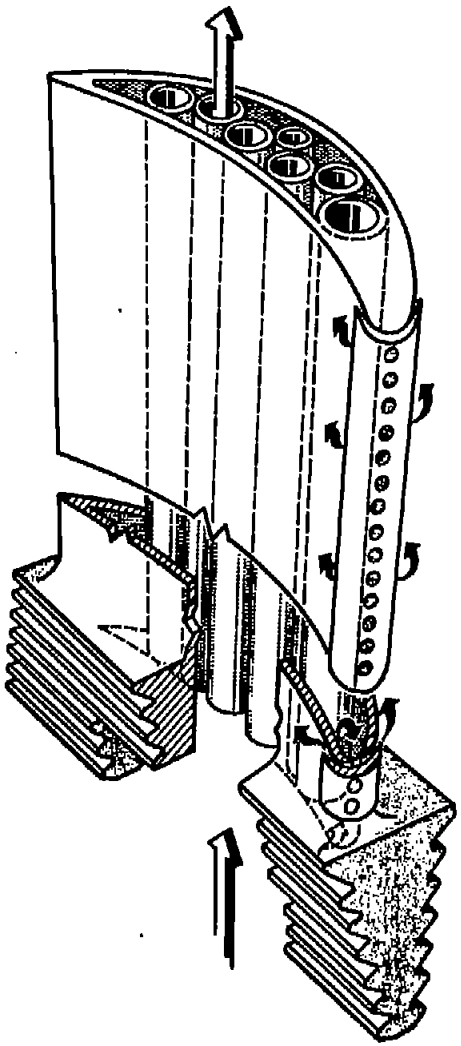

(a) Coolant flow path and structural detail.

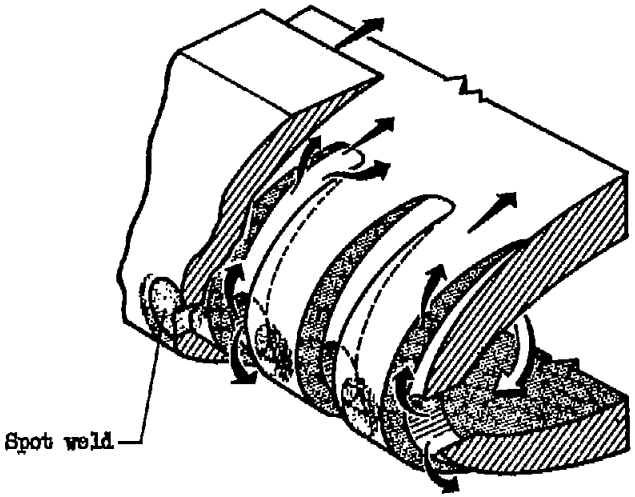

(b) Detail of leading-edge cap.

Figure 1. - Internal coolant passage configuration and structural detail of blade 15.

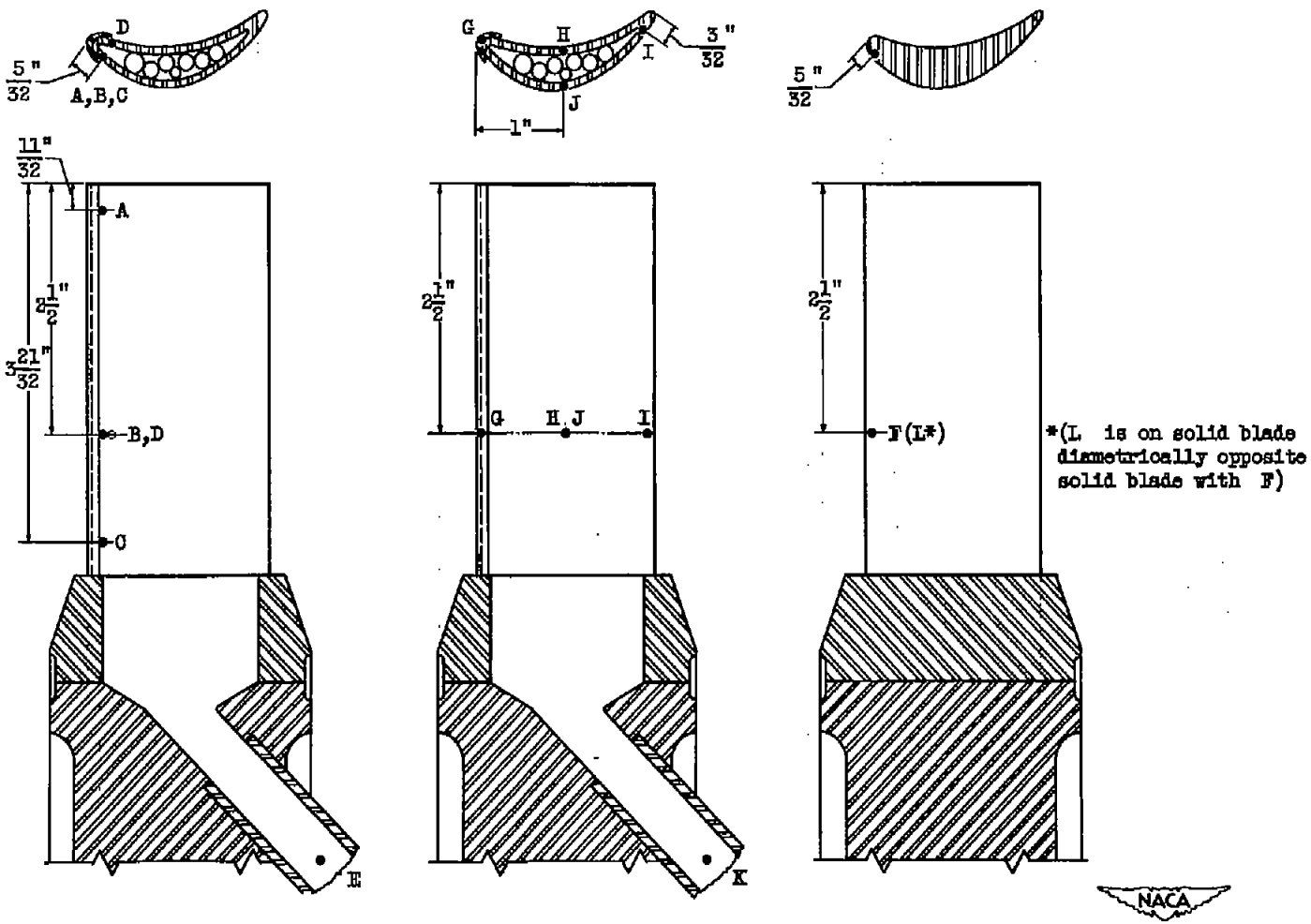

(a) Cooled blades.

(b) Uncooled Blade.

Figure 2. - Schematic diagram of thermocouple locations on cooled and uncooled blades.

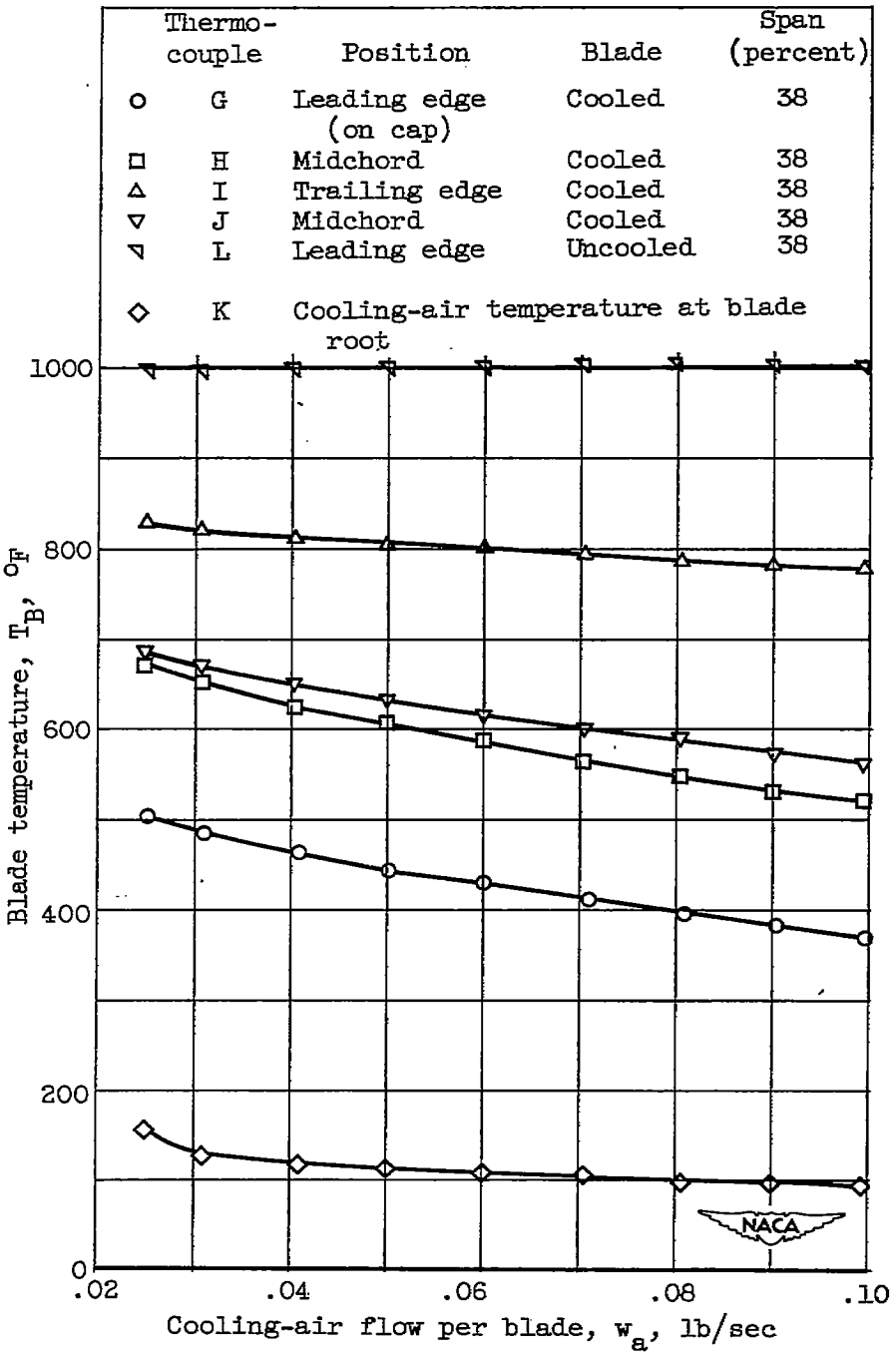

(a) Thermocouples G, H, I, J, K, and L; engine speed, 10,000 rpm.

Figure 3. - Effect of cooling-air flow rate on blade and cooling-air temperatures for blade 15.

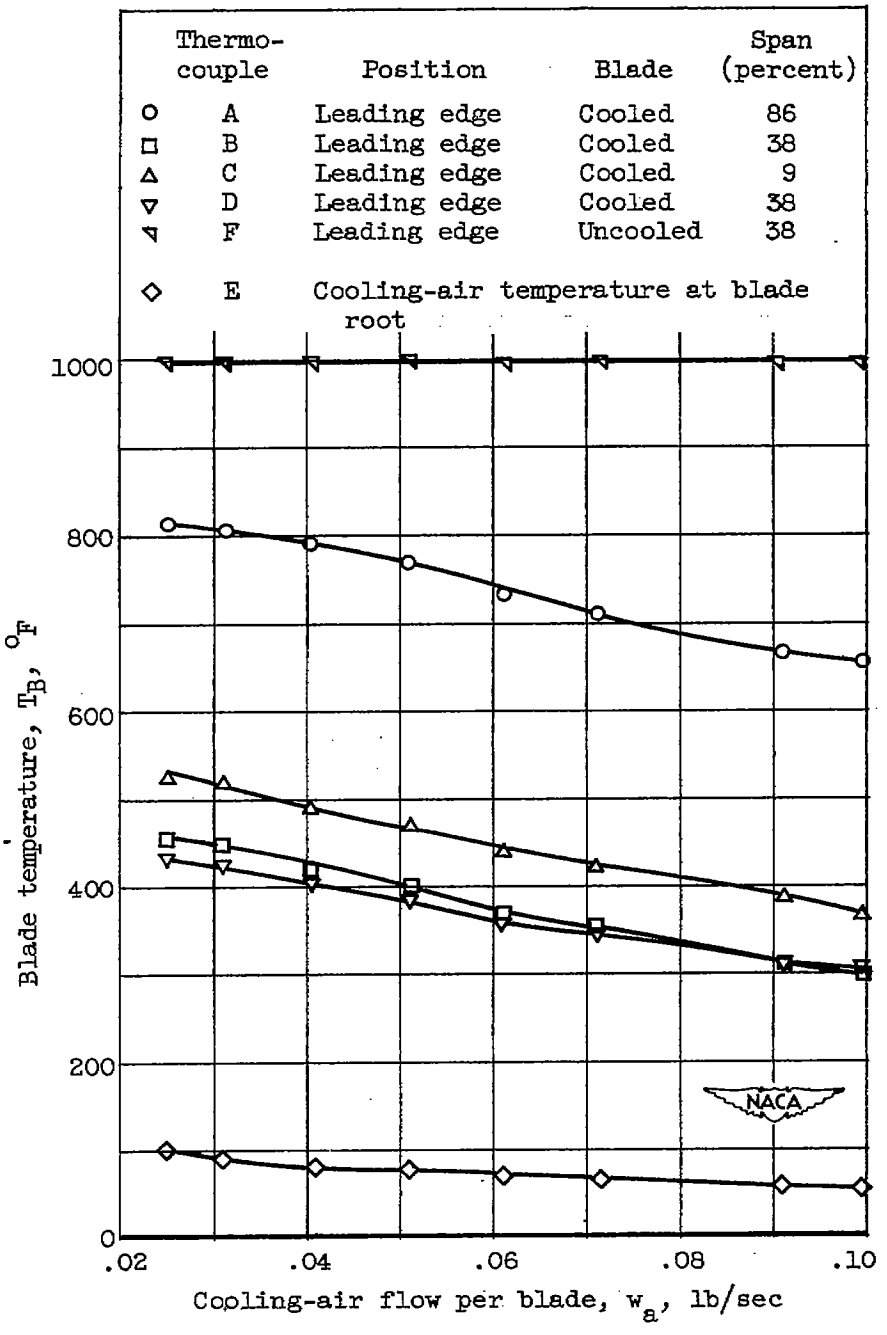

(b) Thermocouples A, B, C, D, E, and F; engine speed, 10,000 rpm.

Figure 3. - Concluded. Effect of cooling-air flow rate on blade and cooling-air temperatures for blade 15.

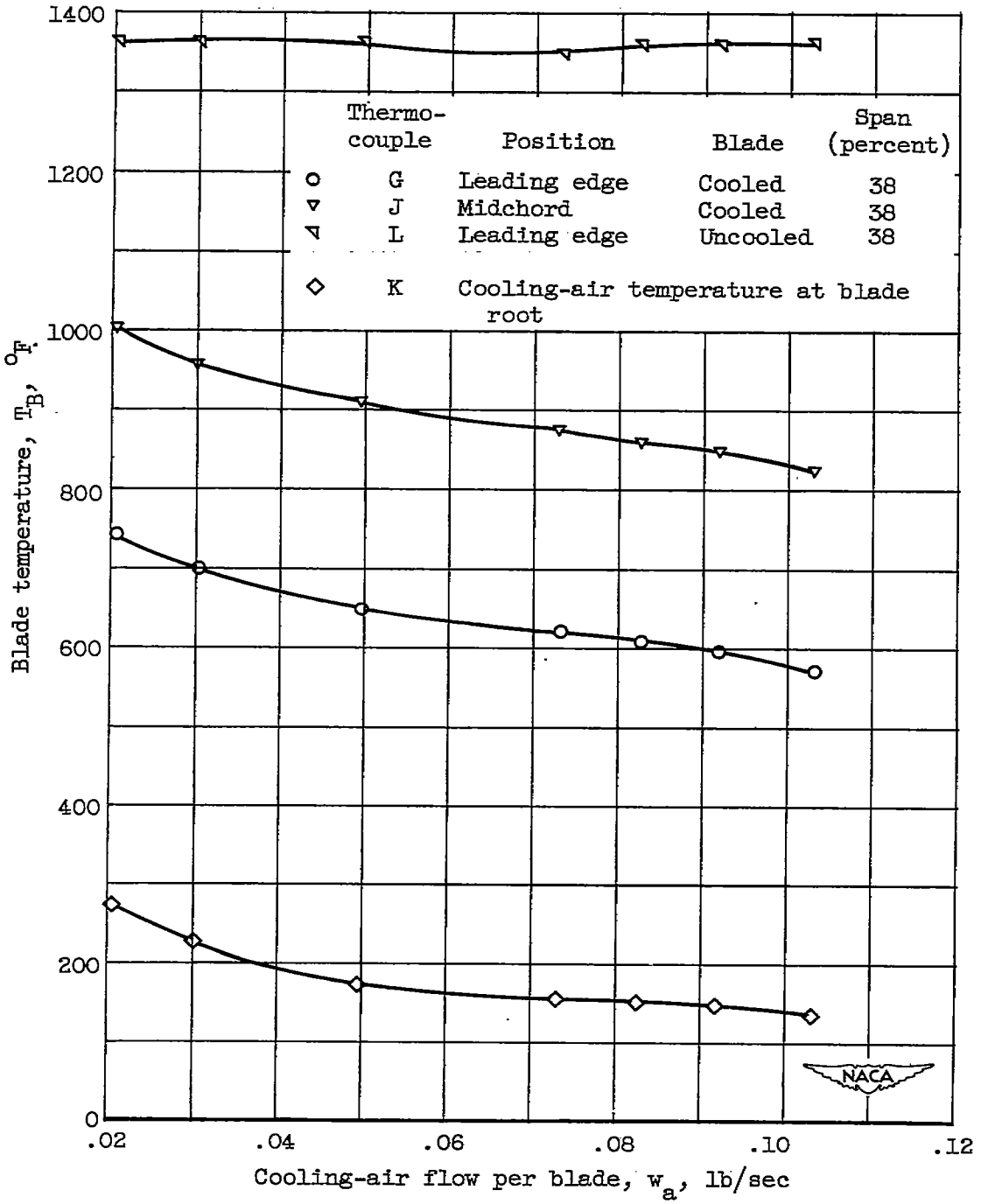

Figure 4. - Effect of cooling-air flow rate on blade and cooling-air temperatures for blade 15 at engine speed of 11,350 rpm.

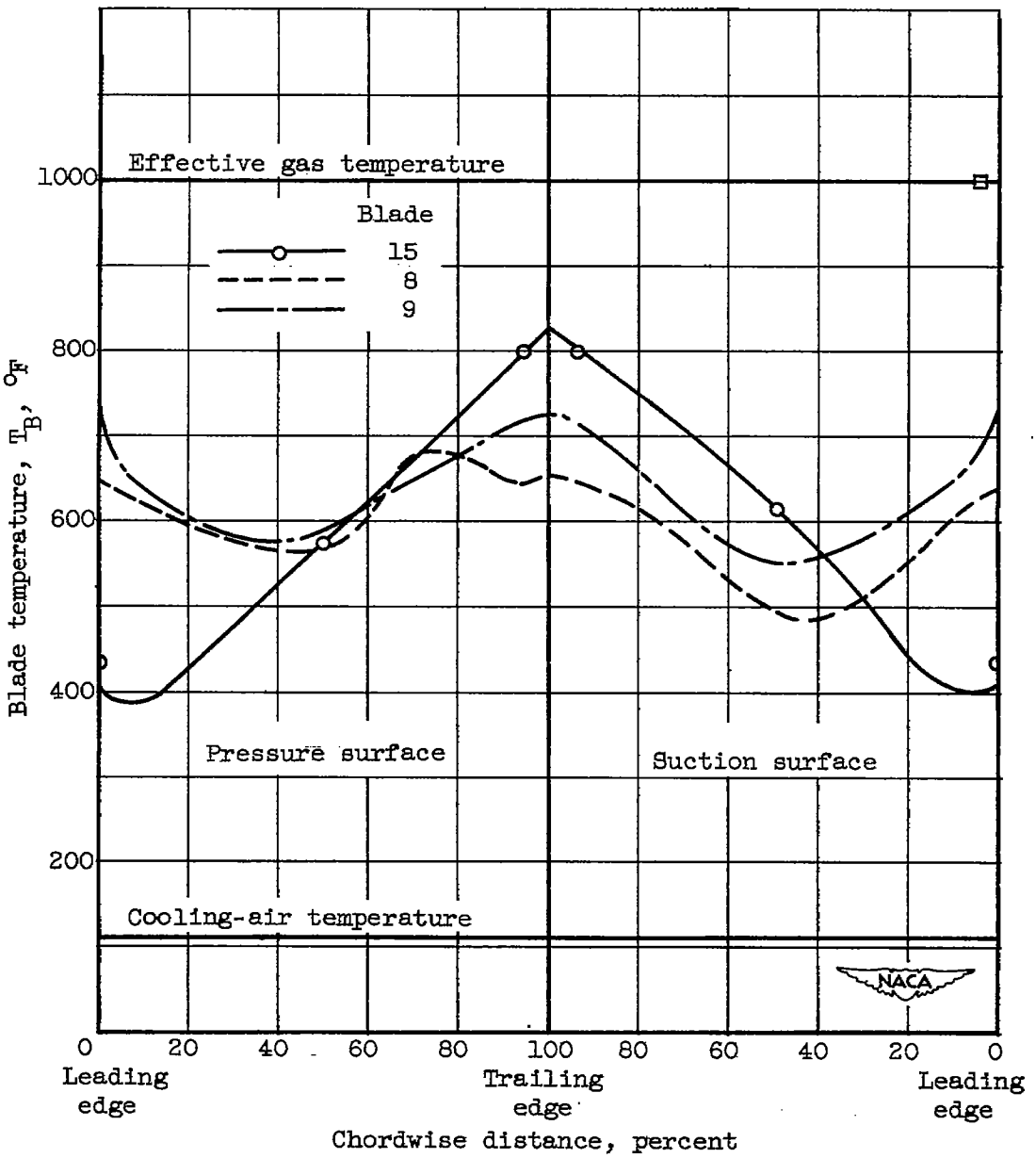

Figure 5. - Comparison of chordwise temperature distributions at 38-percent span location. Coolant flow ratio, 0.054; effective gas temperature, 1000° F; cooling-air temperature at blade base, 109° F; blades 8, 9, and 15.

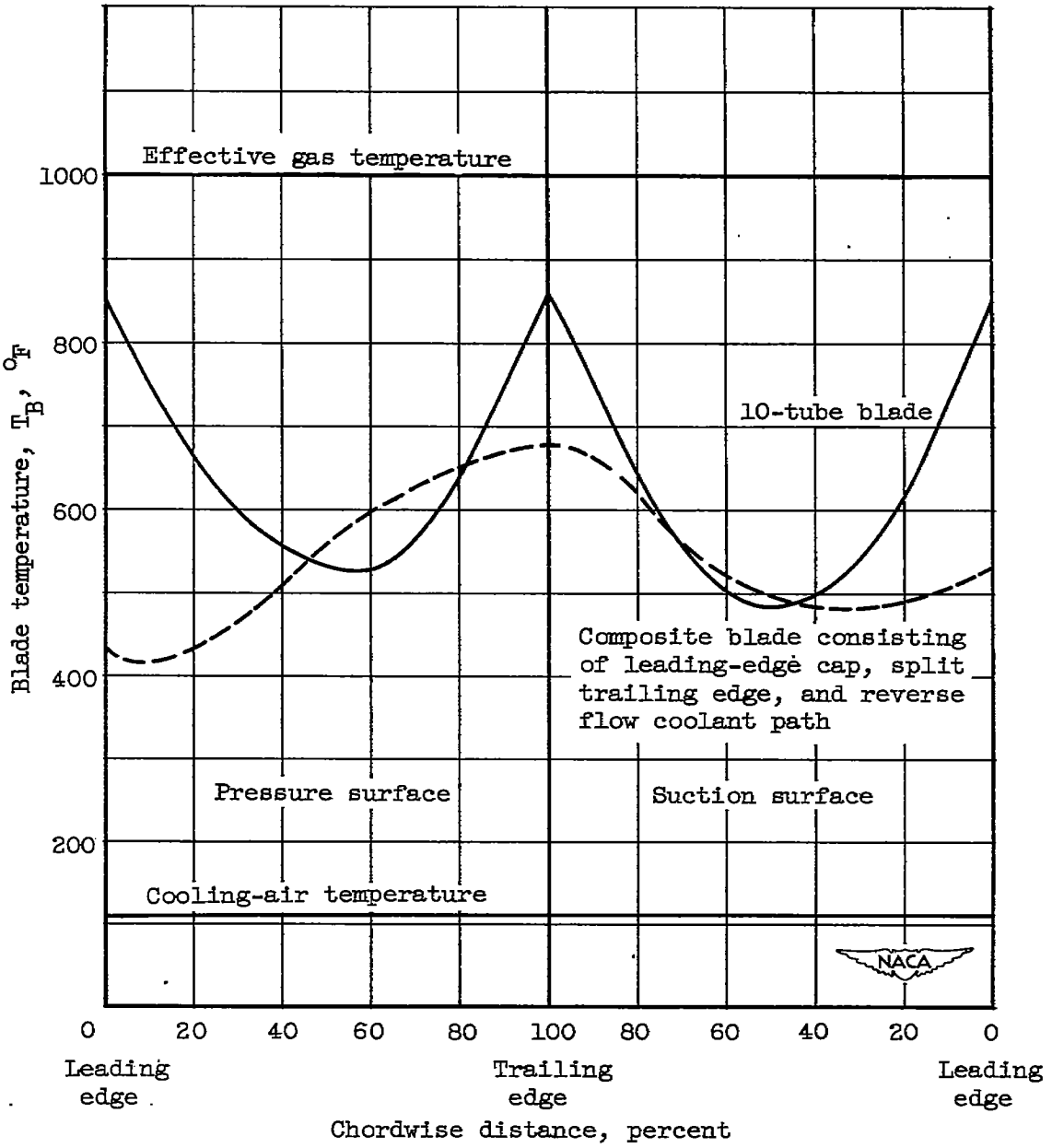

Figure 6. - Comparison of chordwise temperature distributions of hypothetical composite blade and 10-tube blade. Coolant flow ratio, 0.05; engine speed, 10,000 rpm.

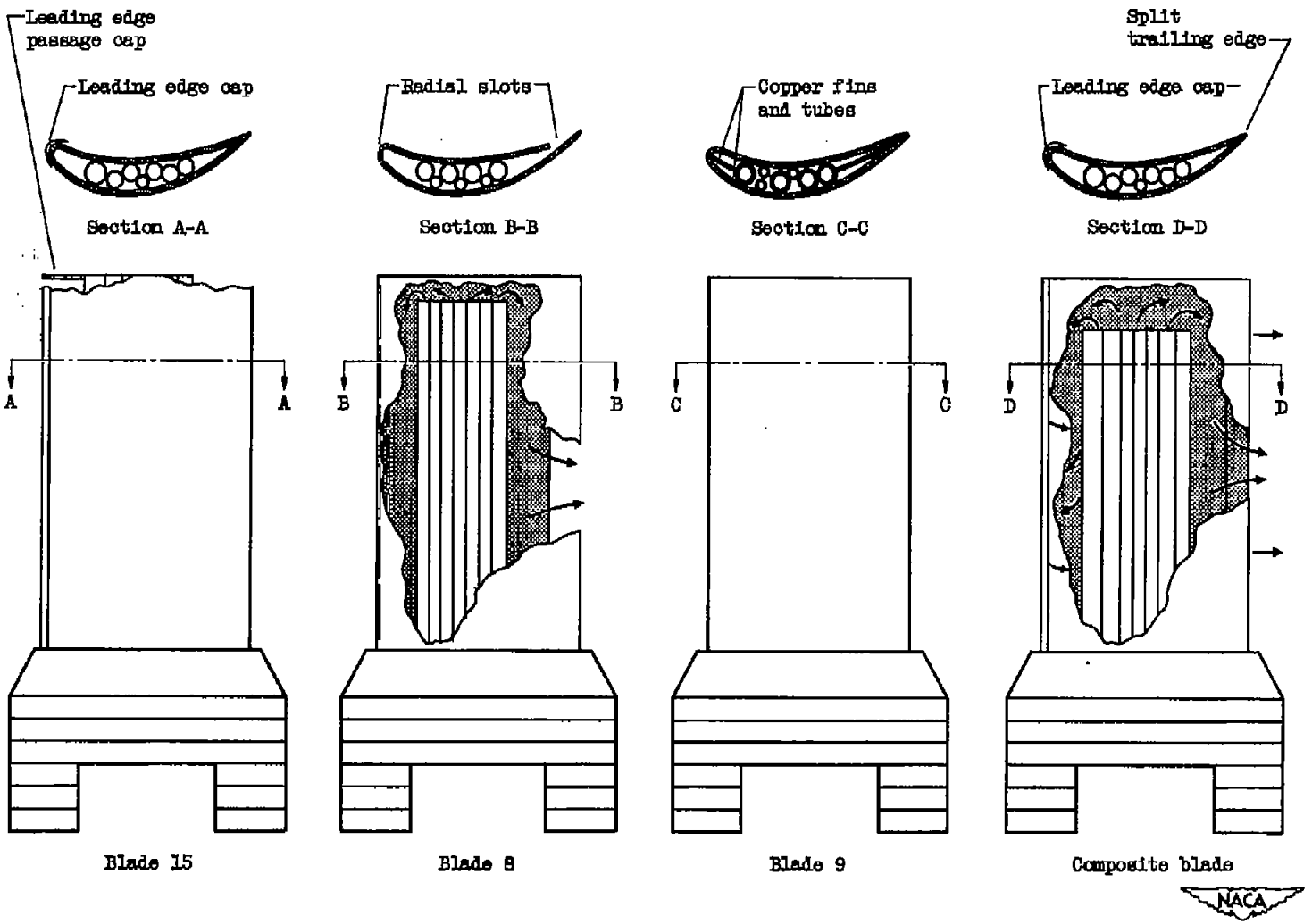

Figure 7. - Comparison of principal design features of blades 15, 8, 9, and composite blade.

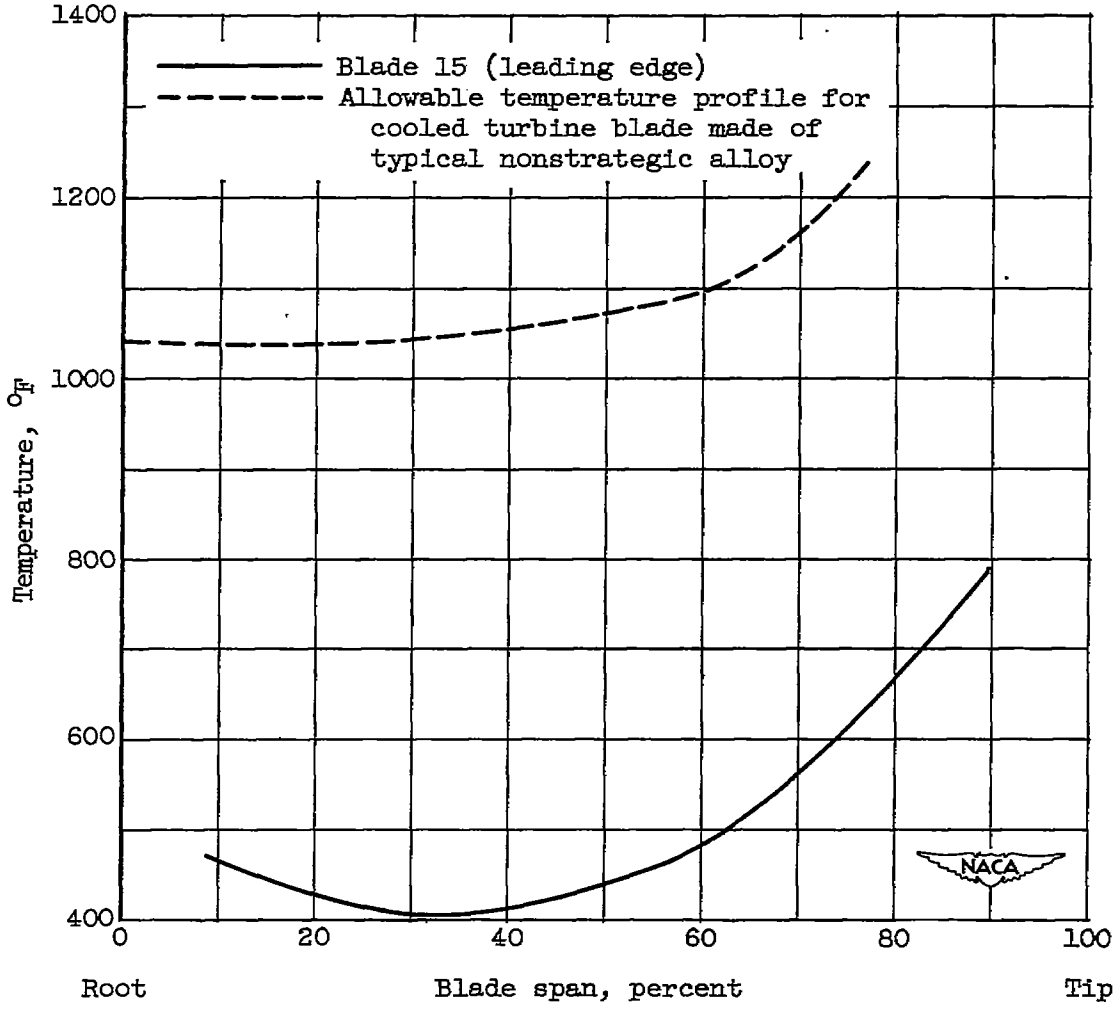

Figure 8. - Spanwise temperature distribution at leading edge of blade 15. Coolant flow ratio, 0.05; effective gas temperature, 1000° F; cooling-air temperature at blade root, 109° F; standard sea-level engine-inlet conditions; engine speed, 10,000 rpm.

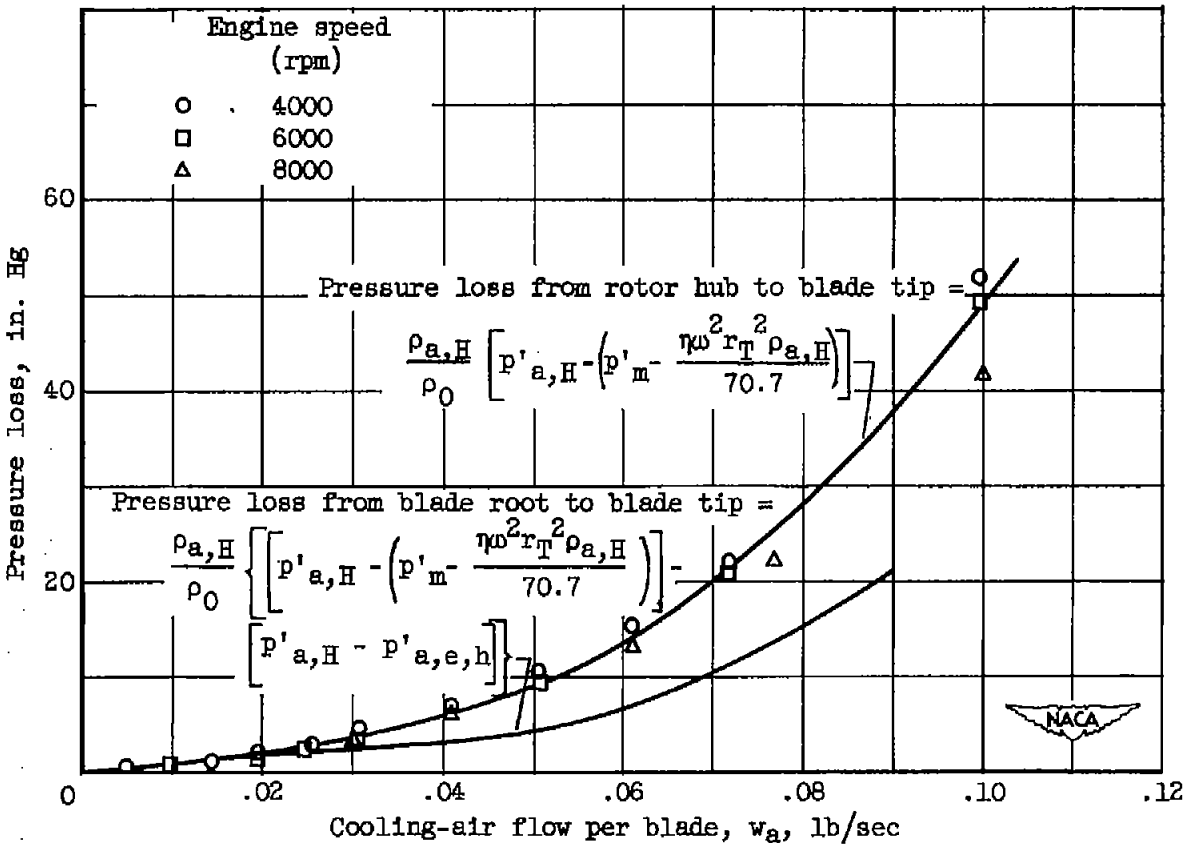

Figure 9. - Correlation of pressure loss from rotor hub to blade tip and from blade root to blade tip.

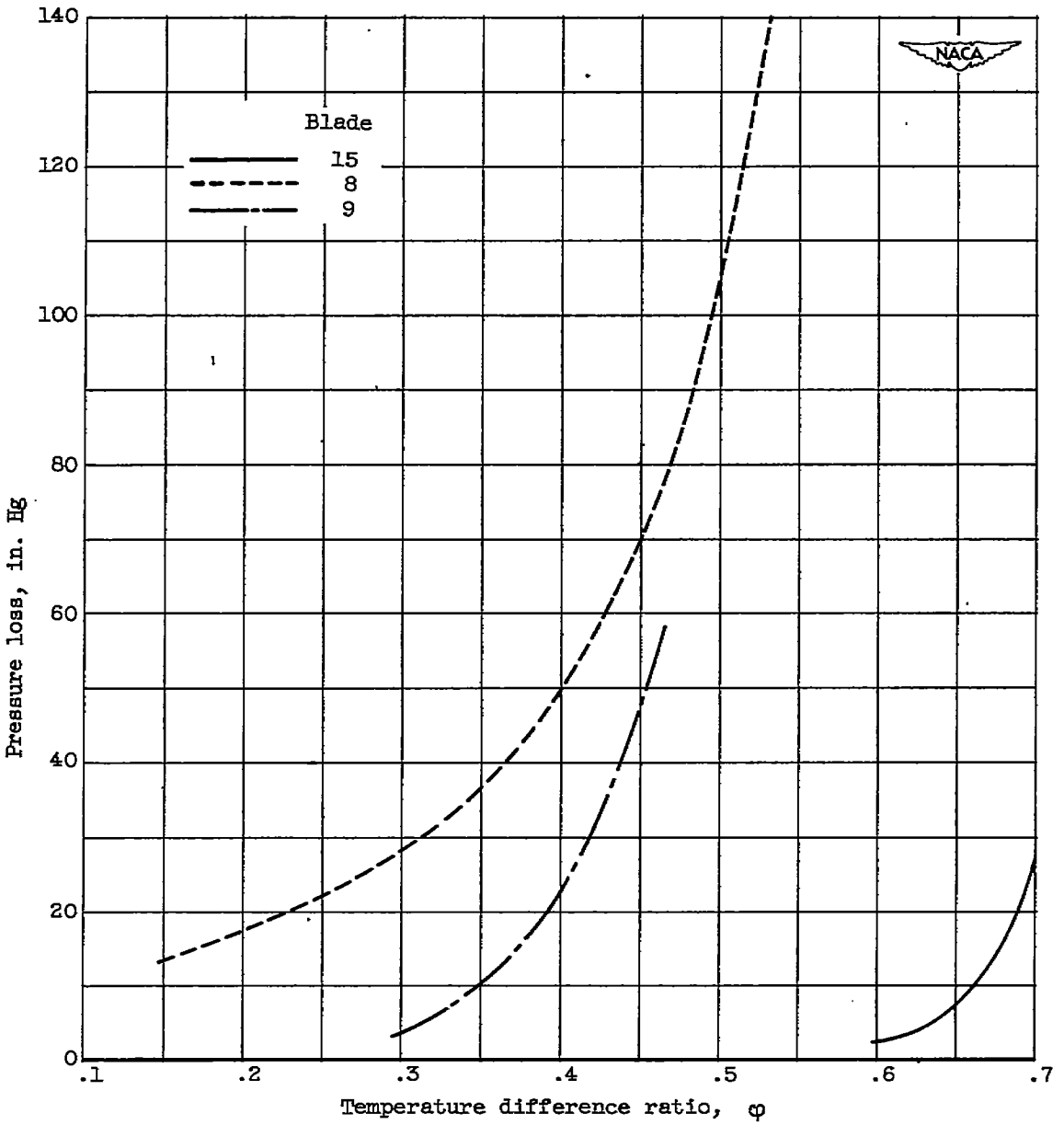

Figure 10. - Comparison of pressure loss required by blades 8, 9, and 15 for range of cooling effectiveness. Thermocouple G; engine speed, 10,000 rpm.